



## 3D heterogeneous islet organoid generation from human embryonic stem cells using a novel engineered hydrogel platform



Joseph Candiello<sup>a</sup>, Taraka Sai Pavan Grandhi<sup>b,2</sup>, Saik Kia Goh<sup>a</sup>, Vimal Vaidya<sup>c</sup>,  
Maya Lemmon-Kishi<sup>a</sup>, Kiarash Rahmani Eliato<sup>d</sup>, Robert Ros<sup>d</sup>,  
Prashant N. Kumta<sup>a,c,e,f,g,1</sup>, Kaushal Rege<sup>h,1</sup>, Ipsita Banerjee<sup>a,c,g,\*</sup>

<sup>a</sup> Department of Bioengineering, University of Pittsburgh, PA, United States

<sup>b</sup> Biomedical Engineering, Arizona State University, Tempe, AZ, United States

<sup>c</sup> Department of Chemical and Petroleum Engineering, University of Pittsburgh, PA, United States

<sup>d</sup> Department of Physics, Center for Biological Physics, and Biodesign Institute, Arizona State University, Tempe, AZ, United States

<sup>e</sup> Department of Mechanical Engineering and Material Science, University of Pittsburgh, PA, United States

<sup>f</sup> Center for Complex Engineered Multifunctional Materials, University of Pittsburgh, PA, United States

<sup>g</sup> McGowan Institute for Regenerative Medicine, University of Pittsburgh, PA, United States

<sup>h</sup> Chemical Engineering, Arizona State University, Tempe, AZ, United States

### ARTICLE INFO

#### Article history:

Received 10 May 2018

Accepted 19 May 2018

Available online 25 May 2018

#### Keywords:

Islet

Human embryonic stem cells

Organoid

Hydrogel

Aggregation

Three dimensional

### ABSTRACT

Organoids, which exhibit spontaneous organ specific organization, function, and multi-cellular complexity, are in essence the *in vitro* reproduction of specific *in vivo* organ systems. Recent work has demonstrated human pluripotent stem cells (hPSCs) as a viable regenerative cell source for tissue-specific organoid engineering. This is especially relevant for engineering islet organoids, due to the recent advances in generating functional beta-like cells from human pluripotent stem cells. In this study, we report specific engineering of regenerative islet organoids of precise size and cellular heterogeneity, using a novel hydrogel system, Amikagel. Amikagel facilitated controlled and spontaneous aggregation of human embryonic stem cell derived pancreatic progenitor cells (hESC-PP) into robust homogeneous spheroids. This platform further allowed fine control over the integration of multiple cell populations to produce heterogeneous spheroids, which is a necessity for complex organoid engineering. Amikagel induced hESC-PP spheroid formation enhanced pancreatic islet-specific Pdx-1 and NKX6.1 gene and protein expression, while also increasing the percentage of committed population. hESC-PP spheroids were further induced towards mature beta-like cells which demonstrated increased Beta-cell specific INS1 gene and C-peptide protein expression along with functional insulin production in response to *in vitro* glucose challenge. Further integration of hESC-PP with biologically relevant supporting endothelial cells resulted in multicellular organoids which demonstrated spontaneous maturation towards islet-specific INS1 gene and C-peptide protein expression along with a significantly developed extracellular matrix support system. These findings establish Amikagel –facilitated platform ideal for islet organoid engineering.

© 2018 Elsevier Ltd. All rights reserved.

### 1. Introduction

Degenerative diseases and end-stage organ failure can be effectively treated by transplantation of donor organs. However, a critical shortage of donor tissue has ignited the search for alternate

organ and tissue sources including from human pluripotent stem cell (hPSC) derived tissues. A synergistic goal is to develop model organs from hPSCs for drug screening and toxicity testing. A critical challenge to both these goals is to determine robust means of replicating the organ function, multicellular complexity, and three dimensional (3D) cellular organization in an *in-vitro* setting, which is the goal of current research on organoid generation [1]. An initial success in organoid engineering can be considered to be embryoid bodies derived from murine and human embryonic stem cells (ESC) that demonstrate both germ layer commitment and spatial patterning reminiscent of developing embryos [1]. More recently, organ-specific organoids, have been derived from both mouse and

\* Corresponding author. Department of Chemical and Petroleum Engineering, University of Pittsburgh, PA, United States.

E-mail address: [ipb1@pitt.edu](mailto:ipb1@pitt.edu) (I. Banerjee).

<sup>1</sup> Authors contributed equally to manuscript.

<sup>2</sup> Present address: Advanced Assays Group, Functional Genomics, Genomic Institute of Novartis Research Foundation, La Jolla, CA.

human pluripotent stem cells (PSC) [2–5]. hPSCs have been utilized to derive organoids of endoderm lineage, including intestinal [6], liver [7,8], and kidney organoids [9].

An equivalent hPSC-derived pancreatic islet organoid will have inherent therapeutic potential and usefulness in drug discovery applications relevant to diabetes. Critical shortage of donor islets is currently limiting the widespread implementation of islet transplantation to treat Type-1 diabetes [10]. In response to these needs, recent studies have demonstrated the feasibility of *in vitro* generation of functional islet  $\beta$ -cells from human pluripotent stem cells (hPSCs) as an alternative to donor islets [11,12]. While current studies on regenerative islets primarily focus on deriving islet beta cells, the non-endocrine component of the islet also plays a critical role in its function. Heterogeneous multi-compositional pancreatic organoids generated by aggregating adult mouse  $\beta$ -cell line with endothelial and mesenchymal cells were found to successfully integrate with host vasculature and restore normalization of blood glucose in diabetic mouse models [13]. Thus, for systematic generation of heterogeneous organoids, there is a need for 3D culture platforms which increase cell to cell communication, allow integration of supporting cell populations and facilitate functional maturation [14]. Our objective in this study is to engineer heterogeneous endothelialized 3D islet organoids from hPSC derived pancreatic islet cells utilizing a synthetic biomaterial-based platform, paving the way for next-step generation of entire multi-compositional islet organoids. We generated islet organoids using alternate islet differentiation protocols, thereby demonstrating the broad applicability of the platform.

The development of an *in vitro* organoid system requires key elements of both an organ-specific cell source as well as a platform to induce self-organization and lineage specification [1]. With regards to a regenerative cell source for pancreatic islets, various research groups including ours have demonstrated the successful differentiation of hESCs to pancreatic progenitor lineage using a multi-step directed differentiation approach [15–23]. Design of specific platforms for organoid generation, however, have largely been adopted from existing tissue engineering platforms. Existing systems include scaffold-free platforms which force aggregation of the cell population [2,5,24,25]. Scaffold-based strategies have primarily relied on laminin-rich matrigel [1,3,6] and other natural or synthetic biomaterials [26–31], which typically confine the cell populations within the 3D biomaterial scaffolds. Specific to islet organoids, hPSCs have been aggregated into homogenous, 3D, islet-like spheroids using 2D non-adherent culture [32,33] and embedment in collagen/matrigel matrix [34]. Takebe et al. demonstrated the advantages of heterogeneous pancreatic organoids with a murine  $\beta$ -cell line; in their study, self-organization of multicellular ‘organ bud’ constructs on Matrigel was sensitive to cell density and presence of a stromal cell population [8,13]. Hence, there is a need for robust bio-engineered platforms tailored specifically for organoid production, allowing fine control over organoid size and cellular composition, scaling up of production towards meeting the biomanufacturing goals, and offering ease of organoid recovery after culture.

In this study, we describe a novel hydrogel (Amikagel)-based platform, which promotes spontaneous, rather than forced, aggregation of hESC-derived pancreatic progenitor cells (hESC-PPs) into robust spheroids tunable specifically for size and heterogeneous cellular composition. Compared to the gold-standard Matrigel, integration of the Amikagel platform resulted in significant enhancement of islet phenotype; self-organization into 3D spheroids on Amikagel significantly increases the expression of pancreatic markers Pdx-1 and NKX6.1, along with enrichment of cell populations co-expressing both, indicating a population more primed for islet maturation. Amikagel enabled co-aggregation of hESC-PP with developmentally relevant endothelial cells resulted in self-organized

multicellular pancreatic organoids which are closer to islet physiology in its heterogeneity, as compared to hPSC-PP homogenous spheroids [14]. Amikagel-induced hESC-PP spheroids and heterogeneous organoids could be further induced to differentiate towards mature beta-like cells that show INS1 gene expression as well as C-peptide protein expression. Specifically, the pancreatic islet ‘organoids’ spontaneously matured into beta-like cells in the absence of specific chemical induction. After maturation, the Amikagel induced hESC-PP spheroids demonstrated mature islet function of glucose stimulated insulin secretion (GSIS) *in-vitro*.

## 2. Methods

Detailed experimental methods section included in supporting information.

### 2.1. Amikagel synthesis

Amikacin hydrate (AH) (referred to as amikacin henceforth) and poly(ethyleneglycol) diglycidyl ether (PEGDE) ( $M_n = 500$  Da) were purchased from Sigma-Aldrich (St. Louis, MO), and used without further purification. 20 mL scintillation vials were purchased from Thomas Scientific (Swedesboro, NJ). Ring-opening polymerization between amine groups of amikacin hydrate and epoxide groups of poly(ethylene glycol) diglycidyl ether (PEGDE) resulted in the formation of a novel hydrogel henceforth called ‘Amikagel’. Different stoichiometric ratios of amikacin and the cross-linker PEGDE were added to a 20 mL scintillation vial and dissolved in Nanopure<sup>®</sup> water by vortexing for 30 s. Fig. 1 shows the monomer composition of Amikagels designated  $AM_{\text{Mole PEGDE} / \text{Mole Amikacin}}^{1.5}$  through  $AM^{4.0}$ . Amikagel pre-gel solutions were filtered through a 0.20  $\mu\text{m}$  filter and 40  $\mu\text{l}$  of the filtrate was added to each well of a 96 well plate. The plates were sealed with paraffin tape (Parafilm, Menasha, WI) and incubated in an oven maintained at 40 °C for 7.5 h. Following gelation, Amikagels were washed with 150  $\mu\text{l}$  Nanopure<sup>®</sup> water for 12 h, in order to remove traces of unreacted monomers. All cell culture experiments were set up by liquid overlay culture.

### 2.2. Amikagel characterization

Amikagels were prepared as described above. Amikagel stiffness measurements were carried out for each hydrogel composition in Fig. 1C by measuring the complex modulus using a parallel plate rheometer in an oscillatory mode. Sample surface chemistry was analyzed by conducting analysis of the FTIR spectra of freeze dry lyophilized Amikagel.

### 2.3. Atomic force microscope based mechanical characterization

Force indentation curves were recorded with a commercial atomic force microscope (MFP-3D-BIO AFM, Asylum Research, Santa Barbara CA, USA) using spherical borosilicate beads (10  $\mu\text{m}$  diameter, Thermo Fisher Scientific, Ferreton CA, USA) attached to a tipless cantilever ( $K_{\text{nominal}} = 37$  N/m, Appnano, Mountain View CA, USA). For the quantification of the elastic modulus,  $4 \times 5$  pixel force maps were collected in an area of 90  $\mu\text{m} \times 90 \mu\text{m}$  on the sample surface with indentation speed of 2  $\mu\text{m s}^{-1}$  and a trigger force of 6.5  $\mu\text{N}$ . For dynamic rheology measurements, trigger forces of 2  $\mu\text{N}$  on  $2 \times 5$  pixel force maps were applied. The spring constant of each cantilever was determined by the thermal noise method [35,36]. Two replication experiments were conducted with one sample per condition per experiment. Two force maps per sample were collected. To quantify the elastic moduli the first 5  $\mu\text{m}$  indentation of each force distance curve was fitted to the Hertz model [37]. Complex moduli were obtained by frequency dependent oscillations and collecting

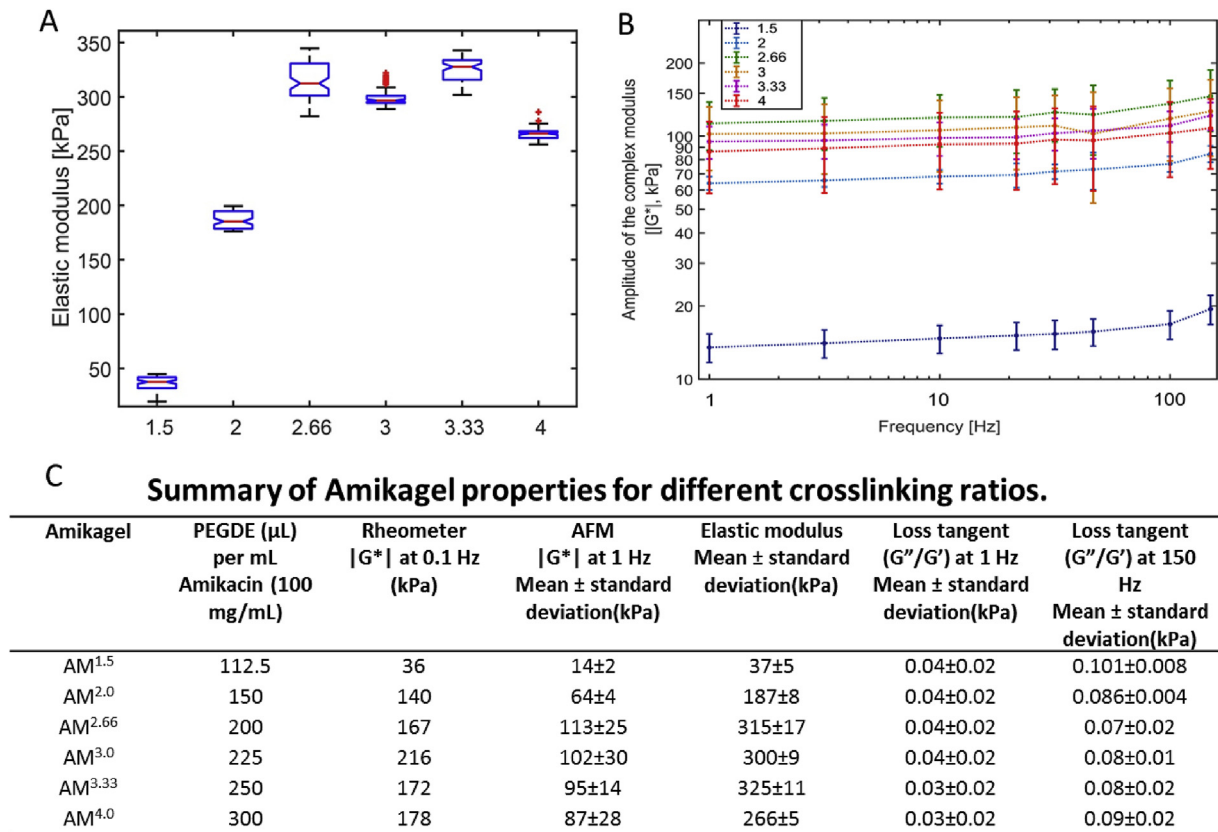


**Fig. 1.** (A) Elastic modulus ( $E$ ) of Amikagels quantified by microrheological AFM using a spherical probe with a diameter of  $10\ \mu\text{m}$  is shown. X-axis shows the ratio of PEGDE:AM used to generate the Amikagels. (B) Elastic modulus ( $E$ ) of Amikagels quantified by microrheological AFM using a spherical probe with a diameter of  $10\ \mu\text{m}$  is shown. X-axis shows the ratio of PEGDE:AM used to generate the Amikagels, (C) Summary of Amikagel Properties for different PEGDE crosslinking ratio.

indentation and force responses of the sample and the phase lag between them. Later, these amplitudes and frequency-dependent version of the Hertz model [38] were used to calculate the complex modulus. For the data analysis MATLAB (version, 9.1) was used. The Poisson's ration of the gel was assumed to be  $\nu_{gel} = 0.5$ .

#### 2.4. Cell culture and hESC differentiation

H1 human embryonic stem cells were used in throughout this study. Two-dimensional differentiation from hESC to hESC-Pancreatic Progenitor cell populations was performed using two independent previously published differentiation protocols [11,39]. Organoids were generated at hESC, hESC-DE, and hESC-PP stage as well as a co-culture of HUVEC and hESC-PP cells (Fig. 2). Single cell suspensions were counted and dispersed in base media supplemented with 2% FBS at desired concentrations for seeding onto Amikagels formed in each well of a 96 well-plate (Fig. 1). For Matrigel controls, single cell suspension was seeded onto TCP coated in thin layer of Matrigel. After aggregation on the underlying Amikagel, chemical maturation was continued by following previously published differentiation protocols [11,39].

#### 2.5. Linescan imaging and aggregation index quantification

GFP-expressing hESC cells were harvested at self-renewal, hESC-DE, and hESC-PP stage and seeded on AM<sup>2.0</sup>, AM<sup>3.0</sup>, and AM<sup>4.0</sup> at a concentration of 200,000 cells per ml, or 30,000 cells per well. After 16 h, fluorescence images were taken at each stage of maturation across Amikagel conditions with an Olympus IX-81 fluorescence microscope. The linescan function of MetaMorph microscopy

software was used to collect the averaged (50 line) fluorescence intensity across each cell population. The aggregation index (AI) was calculated by the ratio of fluorescence intensity to cell aggregate width. Measurements were made on 4 samples per condition and conditions which resulted in no aggregation were not quantified.

Brightfield images taken with Olympus IX-81 immediately after organoid formation were analyzed using MetaMorph software at hESC-PP seeding densities of 2000 to 30,000 cells. For each seeding concentration  $n = 10$  images were measured to determine the average diameter relative to starting cell population. Organoid circumferences were tracked in a similar manner by subsequent brightfield imaging from day 1 to day 6.

#### 2.6. Time lapse imaging and condensation quantification

Brightfield images were acquired using an Olympus IX-81 microscope during organoid formation. Time lapse images were acquired starting at initial Amikagel cell seeding until organoid formation was complete ( $t = 16\ \text{h}$ ) at an interval of 15 min. Temperature and  $\text{CO}_2$  homeostasis was maintained at  $37\ ^\circ\text{C}$  and 5%, respectively, using a stage top incubator unit (Tokai Hit, Japan). During co-culture experiments either the HUVEC or hESC-PP cells were pre-labeled with DiD live cell tracking dye to verify population integration during organoid formation. Time lapse images were compiled using MetaMorph software to generate representative movies for organoid formation.

Time lapse organoid images were further analyzed using a previously published macro [1] and method [13] to determine the outline edge (L) and total projected area (A) at each time point as the organoids began to coalesce. The radial edge distance defined as

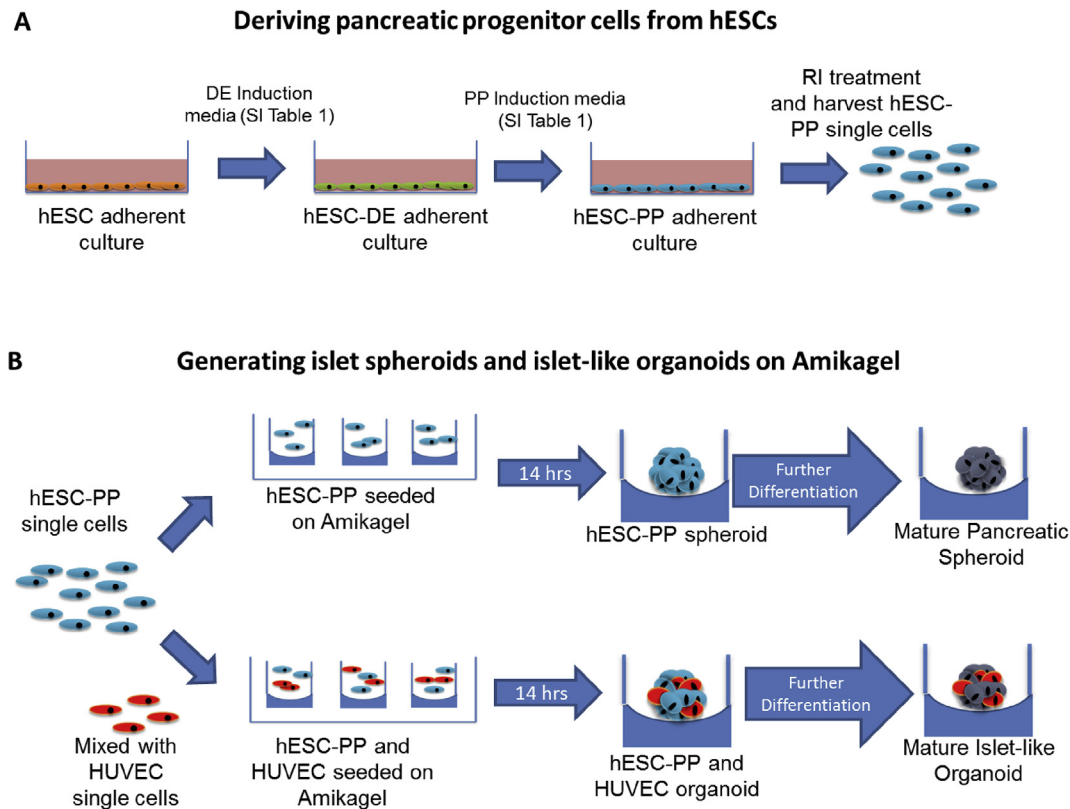


**Fig. 2.** Schematic of fabrication processes for hESC derived islet homogenous spheroids and endothelialized heterogeneous organoids. (A) hESCs are pre-differentiated on 2D matrigel to generate hESC-pancreatic progenitor cells (hESC-PPs). (B) Harvested hESC-PPs are seeded onto individual wells of a 96-well plate containing Amikagel hydrogel platform for spheroid formation combined with endothelial (HUVEC) cells to form heterogeneous islet-like organoids. Media components are listed in [SI Table 1](#).

$A/\sqrt{\pi}$  and circularity defined as  $C = 4\pi A/L^2$  were determined at  $n \sim 100$  time points for  $n = 3$  organoid repeats. The average of repeats was fit using Graphpad Prism 6 (ordinary, least squares) with Kelvin-Voigt viscoelastic model,  $Y = Ae^{(-t)/\tau} + B$ , previously defined [13]. First derivative curves of the model fit were used to determine the rate of change of the radial aggregation component.

### 2.7. Quantitative reverse-transcription polymerase chain reaction

RNA was extracted from 2D cell (1 well per repeat) and organoid populations (10 organoids per sample) and analyzed as described previously (41, 45). Please reference [SI Materials and Methods for expanded details](#).

### 2.8. Immunostaining whole mount and paraffin sections of organoids

Organoids were harvested and fixed with 4% formaldehyde in PBS solution and suspended in Histogel (Thermo Scientific) prior to paraffin sectioning for immunostaining and imaging on Olympus IX-81 fluorescence microscope or Nikon A1 confocal microscope. For whole mount immunostaining, harvested organoids were placed in chamber slides before confocal imaging with Nikon A1 microscope. Please refer to [SI Materials and Methods for expanded details](#).

### 2.9. Flow cytometry

Flow cytometry was performed as previously described (46) using an Accure C6 flow cytometer. For cell cycle analysis, DNA content histogram for the cellular population was analyzed for the fraction of cellular populations in each phase of cell cycle using Modfit LT. Please reference [SI Materials and Methods for expanded details](#).

### 2.10. In vitro functional insulin secretion assay

Harvested hPSC-PP matured spheroids from two separate maturation trials underwent glucose challenge as previously described [11]. Briefly, spheroids were washed with Krebs buffer then placed in low (2 mM) glucose Krebs for 1 h to remove insulin. Spheroids were washed twice, and incubated in low glucose Krebs for 30 min, and supernatant collected. This was followed by washing and incubated in high glucose Krebs for 30 min, and supernatant collected. Finally, spheroids incubated in Krebs containing 2 mM glucose and 30 mM KCl to depolarize for 30 min, then supernatant collected. Ultrasensitive Insulin ELISA kit (ALPCO) was used to detect levels of insulin secretion.

### 2.11. Statistical analysis

Quantification of data was expressed as mean  $\pm$  one standard deviation (SD). Significant differences among groups were determined by  $t$ -test for two-group comparisons or ANOVA for multiple group comparisons. PCR gene expression and Insulin release assay experiments were carried out with  $n \geq 3$  and flow cytometry groups had cell count of  $n > 10,000$  events. Probability values at  $P < .01$  and  $P < .05$  (\*) designate statistical significance.

## 3. Results

### 3.1. Synthesis of Amikagel with tunable physiochemical properties to drive self-aggregation of hESC derived cells

The hydrogel Amikagel was generated by polymerizing amikacin, an aminoglycoside antibiotic, with PEG-diglycidylether (PEGDE) at 40 °C. The aminoglycoside amikacin contains three hexose rings and four amines in its structure; one of these amines is

a primary aliphatic amine. We used amikacin as one of the monomers for generating the gel because it offers an easy approach to tune the physical and chemical properties of the gel by simply modulating the monomer mole ratio. In addition, the presence of sugar groups, consisting of hydroxyls and amine, in the molecule makes the resulting hydrogel hydrophilic and biocompatible. Amikacin allows crosslinking at room temperature or modestly elevated temperatures such as 40 °C. Even though hydrogel formation is possible at 37 °C, kinetics may be enhanced only by modestly increasing the polymerization temperature to 40 °C. Unlike several other biomaterials and cross linkers, amikacin and diglycidyl ether cross-linking does not require UV light and photoinitiators. The resulting hydrogels (“Amikagels”) facilitate the formation of organoids by aggregation or also separation of heterogeneous populations [40]. Modulation of the monomer conjugation ratio resulted in varying the Amikagel constructs, designated  $AM_{Mole\ PEGDE}^{Mole\ Amikacin}$  (AM<sup>1.5</sup> through AM<sup>4.0</sup>) (Fig. 1), each having unique mechanical and chemical properties that influence cell aggregation. The extent of cross-linking altered Amikagel’s chemo-mechanical properties, including stiffness (Fig. 1), protein adsorption (Fig. 1A), and surface biochemistry/amine content deduced from the FTIR fingerprints analysis (Fig. 1B) which can all significantly influence the cell substrate interaction.

We further carried out an AFM microrheological study and compared these findings with properties obtained using bulk material rheology. Fig. 1A shows the elastic modulus ( $E$ ) quantified by microrheological AFM using a spherical probe with a diameter of 10  $\mu\text{m}$ . We found elastic moduli of  $37 \pm 5$  kPa to  $266 \pm 5$  kPa for Amikagel PEGDE concentrations of 112.5  $\mu\text{L/mL}$  to 300  $\mu\text{L/mL}$ . Fig. 1B shows frequency sweeps (1–150 Hz) of the amplitudes of the shear complex moduli ( $|G^*|$ ), with complex modulus amplitudes at 1 Hz of  $14 \pm 2$  kPa, to  $87 \pm 28$  kPa for the same Amikagel concentrations range. Amikagel samples, at all concentrations that we measured, showed to be predominantly elastic due to their small loss tangent in the range of  $0.03 \pm 0.02$  at 1 Hz to  $0.10 \pm 0.01$  at 150 Hz ( $G''/G'$ , where  $G''$  and  $G'$ , shear loss and storage moduli, are the complex and real component of the  $G^*$ ). Therefore, the relation between elastic and complex shear moduli can be summarized as  $E \approx 2(1 + \nu)G^*$  where  $\nu$  is Poisson’s modulus which we assumed to be 0.5 [41–44]. This relation between elastic and shear modulus holds well within the Amikagel AFM measurements. Complex shear moduli measurements obtained by AFM (Fig. 1) were found to be in the same order of magnitude to those estimated via parallel plate rheology. One should note that in this AFM rheology areas of  $90 \times 90 \mu\text{m}^2$  with the maximum indentation depth of 5  $\mu\text{m}$  were measured, whereas in parallel plate rheology about 1 mm in depth on a much larger area of the samples were probed. This could add effects of stiffness of the deeper layers as parallel plate rheology measures the property of the bulk material whereas microrheological AFM measures surface level stiffness. Our data show that cells at the micro-scale experience the same order of magnitude stiffness as the bulk stiffness.

In addition to substrate properties, cell aggregation is also dictated by the cell adhesion molecules on cell surfaces. Specific to islet development, cadherins play a critical role in aggregation of pancreatic endocrine cells [45]. The cell surface properties of hPSCs are known to change during *in-vitro* differentiation [46]. Specifically, the E-cadherin and N-CAM gene expression increases with differentiation from hESC-DE to hESC-PP (SI Fig. 2) [47]. Hence, we tested the self-aggregation potential of hESCs on the Amikagel derived substrates (Fig. 2) at different stages of hESC to pancreatic progenitor differentiation stage (SI Fig. 3) [15]: (i) after propagation (UD hESCs), (ii) at the Definitive Endoderm stage (hESC-DE) and (iii) at the Pancreatic Progenitor stage (hESC-PP). Cells were harvested from each of these stages, along with control endocrine

(MIN6) and exocrine (AR42J) mature pancreatic cell lines and seeded onto 96 well plates coated with pre-formed AM<sup>2.0</sup>, AM<sup>3.0</sup>, and AM<sup>4.0</sup> Amikagels. At 16 h post-seeding (Fig. 3A, hESC derived cells and Fig. 3B, MIN6 and AR42J cell lines), it was observed that the cell morphology was highly sensitive to both, the stage of differentiation as well as the Amikagel formulation. The state of aggregation for each Amikagel formulation condition was quantified by an aggregation index (AI) metric (Fig. 3C), estimated from the total fluorescent signal (TFS) per aggregate width, determined from the linescan fluorescence profiles.

No cell aggregation was observed on AM<sup>2.0</sup>; instead, scattered single cell morphology was observed consistently across the

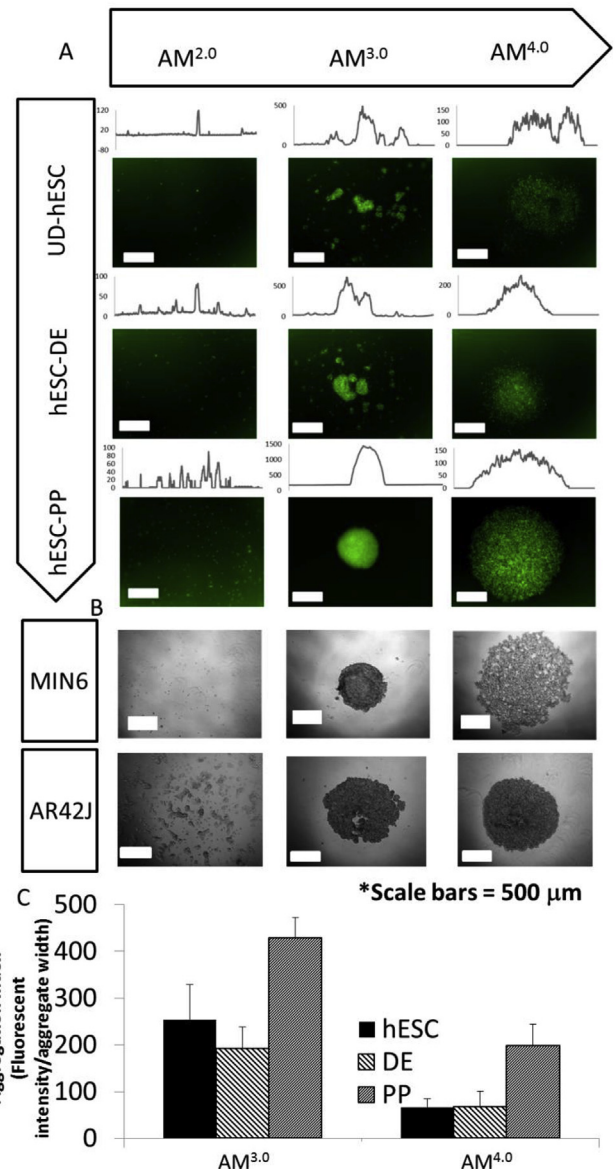


**Fig. 3.** Amikagel substrate with tunable properties can drive aggregation of pre-differentiated hESC cells. (A) Fluorescent images of GFP-labeled hESC and corresponding fluorescent intensity linescan for undifferentiated hESC, hESC-definitive endoderm (hESC-DE), and hESC-pancreatic progenitor (hESC-PP) seeding populations on Amikagel conditions AM<sup>2.0</sup>, AM<sup>3.0</sup>, and AM<sup>4.0</sup>. (B) MIN6 endocrine and AR42J exocrine pancreas cells as controls. (C) Comparison of quantified aggregation index (AI, TotalFluorescent Intensity/mm) from (A) across different Amikagels and at different differentiation stage for those that formed aggregates. Overall hESC-PP cells on AM<sup>3.0</sup> achieved highest AI.

differentiation stages tested (Fig. 3A left panel). Increasing the PEGDE content in the hydrogel led to increased spontaneous aggregation of cells as visualized in Fig. 3A – middle column and quantified by AI. Most dramatic was the aggregation of the hESC-PP cells, which coalesced to form a single compact spheroid, eliciting a significantly higher AI value of  $488 \pm 44$  TFS/ $\mu\text{m}$  which is almost double that of self-renewing hESC, 254 TFS/ $\mu\text{m}$ , and DE, 193 TFS/ $\mu\text{m}$  (Fig. 3C). Importantly, only the hESC-PP seeded on AM<sup>3.0</sup> formed a single uniform aggregate, which was mechanically stable and robust enough to allow for physical manipulation and harvesting (Fig. 4A). This aggregation occurred within 14 h of initial cell seeding (Fig. 4B, Supp movie 1). In order to analyze if the cell aggregation is primarily driven by cell migration, we quantified the kinetics of hESC-PP aggregation and compared it to the rate of cell migration (0.2–0.5  $\mu\text{m}/\text{min}$  [48]). Briefly, we adapted a quantitative image analysis method [13] to track the average spheroid radius change over time (Fig. 4C, SI Fig. 4), from the time-lapse images comprising the initial 18 h of aggregate formation (selected time points Fig. 4B). The average rate of aggregation (ROA) (SI Fig. 4C), decreased from an initial value of 1  $\mu\text{m}/\text{min}$  at 2 h' post seeding on AM<sup>3.0</sup>–0.5  $\mu\text{m}/\text{min}$  at  $t = 4$  h. With further condensation, the aggregation rate decreased to 0.2  $\mu\text{m}/\text{min}$  at  $t = 10$  h before approaching  $\sim 0$   $\mu\text{m}/\text{min}$  as the spheroids compacted. As the AM<sup>3.0</sup> spheroids compacted into a circle (sphere in 3D) the circularity ( $C = \frac{4\pi A}{\text{Perimeter}^2}$ ) increased at  $t = 10$  h as ROA slowed and compaction began and reached a final value of  $\sim 0.8$  at  $t = 14$  h (Fig. 4C). With continued culture on AM<sup>3.0</sup>, the overall spheroid diameter modestly and steadily decreased with culture time, likely due to further compaction (Supp Fig 5). A culture time of 6 days resulted in approximately 10% reduction in spheroid size for each seeding population.

Supplementary video related to this article can be found at <https://doi.org/10.1016/j.biomaterials.2018.05.031>.

While the AM<sup>3.0</sup> gels induced robust aggregation of specifically hESC-PP cells, further increase in PEGDE ratio to AM<sup>4.0</sup> uniformly organized the cells into a single aggregate across all cell types (Fig. 3A – right panel). However, the AI value of the individual aggregates at AM<sup>4.0</sup> (Fig. 3B) were significantly lower than corresponding AM<sup>3.0</sup> values, corresponding to loose aggregation (SI movie 2) which resulted in a decrease in the overall aggregate mechanical stability as well as dissociation during media changes.

Interestingly, with increasing PEGDE concentration to AM<sup>4.0</sup> (Fig. 4C, SI Fig. 4) the initial ROA had a much lower maximum value of  $\sim 0.4$   $\mu\text{m}/\text{min}$  at  $t = 2$  h post seeding that gradually decreased to  $\sim 0.2$   $\mu\text{m}/\text{min}$  at  $t = 10$  h. The AM<sup>4.0</sup> circularity also increased at  $t = 10$  h as ROA slowed, however the maximum circularity factor halted at a value of  $\sim 0.65$  indicating aggregation without further compaction.

Supplementary video related to this article can be found at <https://doi.org/10.1016/j.biomaterials.2018.05.031>.

Thus, only beyond pancreatic commitment (Pdx 1<sup>+</sup>) the hESCs were amenable for robust and reproducible aggregation into single compact spheroid on Amikagel. To determine if this is an endocrine trait, we seeded pancreatic endocrine cell line (MIN6) on Amikagel, which mirrored the aggregation behavior of hESC-PP: no aggregation on AM<sup>2.0</sup>, compact spheroid on AM<sup>3.0</sup>, and loose aggregation on AM<sup>4.0</sup> (Fig. 3B). On the other hand, pancreatic exocrine cells, AR42J, did not exhibit full compaction into 3D spheroids on any Amikagel construct (Fig. 3B). This indicates aggregate formation to be a specific trait of pancreatic endocrine cell-types, in alignment with morphogenic endocrine aggregation events during islet development [45].

Amikagel-induced cell aggregates retained high viability after 5 days of cultures, determined using live/dead assay (Fig. 4D for AM<sup>3.0</sup>, SI Fig. 6A for other Amikagels) and LDH cell death assay (Supp Fig 6B). Importantly, the AM<sup>3.0</sup> platform allowed for consistency and precision in controlling the spheroid size by varying the initial cell seeding density. Aggregates formed from 30 k cells/well, 15 k cells/well, 7.5 k cells/well, and 2 k cells/well (in a 96 well plate) resulted in initial diameters of  $485 \pm 24$   $\mu\text{m}$ ,  $353 \pm 9$   $\mu\text{m}$ ,  $263 \pm 13$   $\mu\text{m}$ , and  $176 \pm 10$   $\mu\text{m}$ , respectively, as illustrated in Fig. 4E.

The above results demonstrate Amikagel (AM<sup>3.0</sup>) to be an effective controlled platform to induce robust aggregation of hESC-PP cells into compact 3D aggregates of tunable size which maintained high viability, mechanically stability, and allowed harvesting for further downstream application.

### 3.2. Generating islet organoids by integrating multiple cell populations on Amikagel

An important characteristic of organoids is their multi-cellular makeup, which closely mimics the native organ or tissue

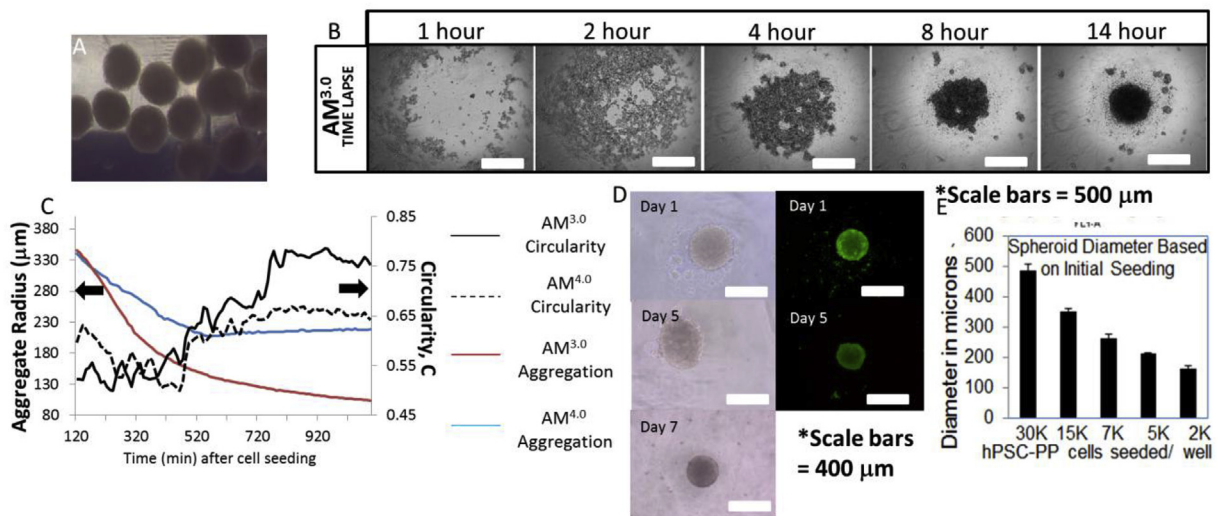


**Fig. 4.** hESC-PP spheroid characterization after spontaneous aggregation via Amikagel. (A) hESC-PP spheroids were mechanically stable to be harvested and cultured in suspension. (B) Selected time lapse images of hESC-PP aggregation on AM<sup>3.0</sup>. (C) Quantified radial aggregation and circularity dynamics for hESC-PP spheroid generation on AM<sup>3.0</sup> and AM<sup>4.0</sup>. (D) Live/Dead spheroid viability assay at day 1 and day 5 after aggregation. (E) Spheroid diameter can be controlled by initial cell seeding population.

composition. In the context of pancreatic islets, a primary non-endocrine component is the endothelial cells constituting the dense intra-islet vascular network. In addition to providing nutritional support, the islet vascular endothelial cells closely interact with endocrine cells during islet development to promote islet maturation via angiocrine signaling [49,50]. In order to reproduce islet constituents in our engineered islet organoids, we co-seeded hESC-PP cells with HUVECs on AM<sup>3.0</sup> gel, on which the cells spontaneously co-aggregated into multicellular 3D organoids. Individually DiD labeled HUVEC and hESC-PP cells verified that both populations were integrated into the multicellular islet organoids (Fig. 5A). Furthermore, the Amikagel system demonstrated precise control over the ratio of seeded cells integrated into each individual organoid (Fig. 5B). DiD labeled hESC-PP cell populations of increasing ratios (0%, 5%, 10%, 25%, 50%, 75%, 100%) were aggregated with unlabeled cells by seeding onto Amikagel hydrogels (Fig 5B top). Quantification of DiD signal using LICOR imaging system demonstrated that the cellular heterogeneity of the ultimate 3D organoids can be controlled through the initial seeding population (Fig. 5B).

The aggregation dynamics of the hESC-PP and HUVEC organoid were determined from time lapse images over the first 18 h of aggregate formation as described in previous sections (selected time points are shown in Fig. 5A). The addition of an endothelial cell population on AM<sup>3.0</sup> decreased the initial rate of aggregation (ROA) at t = 2 h from 1 μm/min for hESC-PP to ~0.65 μm/min in the co-culture (Fig. 5C, SI Fig. 4B and D). At t = 5 h the ROA diminished to 0.5 μm/min, the threshold for cell migration driving aggregation (SI Fig. 4E). The circularity factor increased as ROA slowed, reaching a maximum value of 0.65 (Fig. 5C). These results indicate that the AM<sup>3.0</sup> supported co-aggregation of hESC-PP with endothelial cells, but both ROA and organoid compaction was inhibited in the presence of endothelial cell population.

After an extended 7 day culture period of 1:1 hESC-PP to HUVEC organoids, flow cytometry of the organoids revealed ~45–50% of the cell population to be the hESC-PP cells (Fig. 5D), which is similar to the initial seeding population. Additionally, Von Willebrand Factor (VWF) immunostaining demonstrated a fully integrated HUVEC population throughout the organoid (Fig. 5E).

The above results thus, clearly demonstrate the feasibility of forming multicellular 3D islet organoids from hPSCs on Amikagel. The platform allows control over individual organoid cell population ratios, and the cell populations remained well integrated all through the culture period which are beneficial to engineering a controlled 3D islet configuration.

### 3.3. hESC-PP spheroids on AM<sup>3</sup> enhances pancreatic phenotype

With this novel Amikagel as a potential platform for engineering islet organoids, it is important to evaluate the phenotype and function of the synthesized hESC-PP spheroids post aggregation. hESCs were first induced to pancreatic lineage under adherent culture, as confirmed by gene and protein expression of PDX1 - a key pancreatic transcription factor and strong indicator of the pancreatic progenitor stage (SI Fig. 3 and Fig. 2). hESC-PP cells were subsequently harvested and re-seeded on Amikagel and, in parallel, on Matrigel as a control. Aggregation of these cells on AM<sup>3.0</sup> resulted in a further ten-fold increase in PDX1 expression over the seeded population (Fig. 6A) within 24 h. On the other hand, Amikagel conditions under which the cell did not aggregate, resulted in a reduction in PDX1 expression from the seeded population. This effect is also evidenced in the control cultures on Matrigel, where the cells were predominantly spread out with few regions of micro-clusters observed on the gel (Fig. 6B). Subsequently, only 2–3 fold enhancement in PDX-1 expression was observed on Matrigel, significantly lower than the AM<sup>3.0</sup> cultures. In these cultures, PDX1 protein expression was observed to be primarily localized to

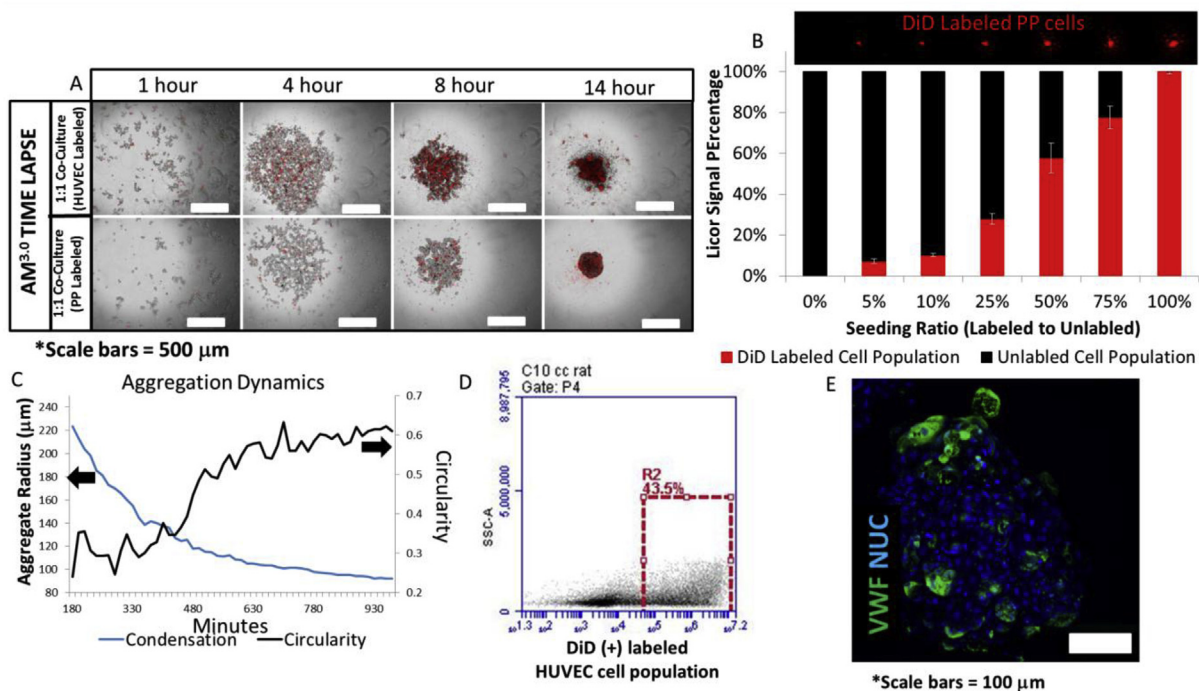


**Fig. 5.** Generation of heterogeneous, multicellular islet organoids on amikagel. (A) Time lapse imaging of co-culture aggregation on AM<sup>3.0</sup> (labeled cell population in red: HUVEC top row and hESC-PP bottom row). (B) LICOR images (top) and quantification (bottom) of DiD labeled to unlabeled cell seeding ratios demonstrated control over mixed cell population inclusion. (C) Condensation dynamics of radial diameter and circularity of co-culture aggregation. (D) Flow cytometry of DiD labeled hESC-PP cells after 7 days of maturation. (E) VWF protein expression of HUVEC distribution in whole mount mature co-culture organoids. Scale bars are 200 μm unless noted. (For interpretation of the references to colour in this figure legend, the reader is referred to the Web version of this article.)

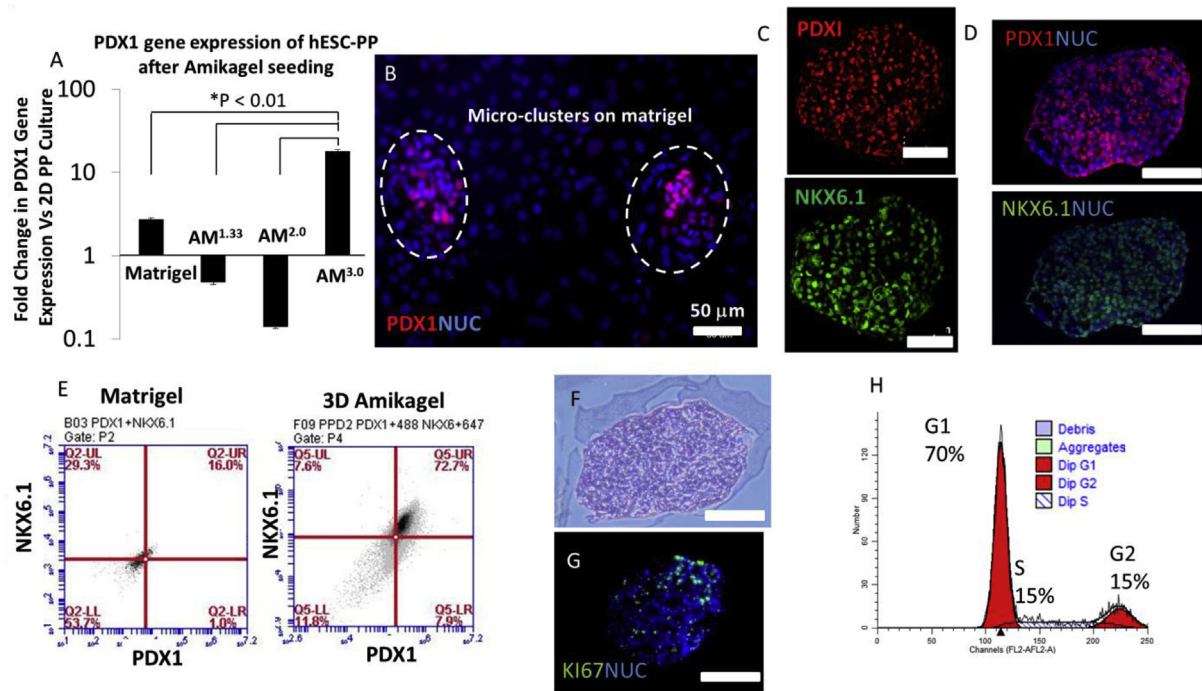


**Fig. 6.** Aggregation of hESC-PP spheroid on AM<sup>3.0</sup> enhances pancreatic phenotype within 24 h after formation. (A) Gene expression of PDX1 across Amikagel conditions and Matrigel control 24 h after seeding. (B) Immunostaining of PDX1 on Matrigel (micro-clusters within circle). (C) PDX1 and NKX6.1 protein expression of whole mount spheroids. (D) PDX1 and NKX6.1 protein expression of hESC-PP spheroid cross-sections. (E) Flow cytometry analysis of the spheroids grown on Matrigel and Amikagel for NKX6.1 and PDX1 co-expressing cell population. (F) Paraffin cross sections of H&E stain (G) KI67 assay detects proliferative cell population. (H) PI staining for cell cycle phase distribution analysis of total hESC-PP cell population after spheroid aggregation. All scale bars in image are 200  $\mu$ m unless otherwise noted.

small regions of 3D micro-clustering (Fig. 6B). Immunostaining of hESC-PP spheroids on AM<sup>3.0</sup> revealed significant positive staining throughout the aggregate for PDX1 and NKX6.1, which are key markers indicative of  $\beta$ -cell specific maturation (Fig. 6C: whole mount; 6D: histology). Additionally, the cell population positive for PDX1 protein increased from ~46.5% (pre-seeding) to ~85% within 36 h of cell aggregation, as determined using flow cytometry (Fig. 6E). Importantly, over 70% of the aggregate cell population co-expressed both PDX1 with NKX6.1 (Fig. 6E). This was a dramatic increase over the control culture where reseeding of the differentiating cells on Matrigel resulted in only 16% of the cell population co-expressing both PDX1 and NKX6.1 (Fig. 6E). Cross-sections of H&E-stained paraffin embedded hESC-PP spheroids (Fig. 6F) demonstrated a uniform cell density across the spheroid, and retained proliferative capability as visualized using KI67 immunostaining (Fig. 6G). hESCs have a unique cell cycle with a brief G1 phase accounting for less than 30% of total cell population. The cell population in the G1 phase increased dramatically with differentiation, which is a hallmark for loss of pluripotency and enhancement of maturation [15]. Flow cytometry analysis of hESC-PP spheroids, 24 h after aggregation, revealed an increase of cell population in the G1 phase to 70%, which is indicative of cell maturation [15] (Fig. 6H). Taken together, the above results uniformly indicate that aggregation of hESC-PP into a compact spheroid on AM<sup>3.0</sup> gels resulted in significant enhancement of pancreatic phenotype, as judged by the PDX1 expression, and enhanced co-expression of PDX1 and NKX6.1, a necessary requirement for beta cell maturation. This effect was significantly higher than parallel control cultures on Matrigel.

#### 3.4. Amikagel enhances maturation and endocrine function of hESC derived islet organoids

The hESC-PP spheroid aggregated on AM<sup>3.0</sup> were further induced towards pancreatic islet lineage by chemical induction.

Differentiated hESC-PP spheroids on Amikagel [51] exhibited approximately 17,000 fold increase in INS gene expression, the hallmark of  $\beta$ -cell maturation, and PDX1 was up-regulated by approximately 7000 fold (Fig. 7A). Parallel cultures on Matrigel control also significantly enhanced the PDX1 and INS gene expression, however corresponding gene expressions of the spheroid cultures on AM<sup>3.0</sup> was 40-fold enhanced over Matrigel control (Fig. 7A). It is well documented that inhibition of Notch signaling by  $\gamma$ -secretase inhibitors are necessary to mature hPSC-PP cells towards  $\beta$ -cell lineage [51]. We further tested here if cell aggregation itself can induce  $\beta$ -cell maturation, in the absence of  $\gamma$ -secretase inhibition. Hence the hESC-PP cells aggregated into 3D spheroids on AM<sup>3.0</sup> were cultured without specific chemical induction for maturation by  $\gamma$ -secretase inhibition. Interestingly, the 3D aggregates showed significant upregulation of PDX1 (16,000 fold) and moderate upregulation of INS1 (4000 fold) (Fig. 7A: (–) DAPT) and Glucagon (Fig S8A) genes over the seeded cell population.

Since aggregation on AM<sup>3.0</sup> was sensitive to the stage of differentiation, we also tested if aggregation was sensitive to the pathway of differentiation. hESCs were differentiated using a recently reported protocol (protocol 2 [17]), harvested at the progenitor stage, aggregated on AM<sup>3.0</sup> and further induced towards maturation. The islet-like spheroids thus obtained, similarly demonstrated a moderate PDX1 upregulation (1200 fold) along with a stronger upregulation on INS (77,000 fold) (Fig. 7A) and Glucagon (Fig S8B) gene expression. Parallel culture of hPSCs as aggregates under stirred suspension was used as the control for this condition. hPSC aggregates differentiated under stirred suspension demonstrated slightly lower levels of PDX1 and INS gene expression (Fig S9), demonstrating that controlled (re-) aggregation of hESC derived pancreatic progenitor population on AM<sup>3</sup> is favorable for islet-specific differentiation.

We have previously reported that paracrine signaling from HUVEC induces insulin gene and protein expression in adherent

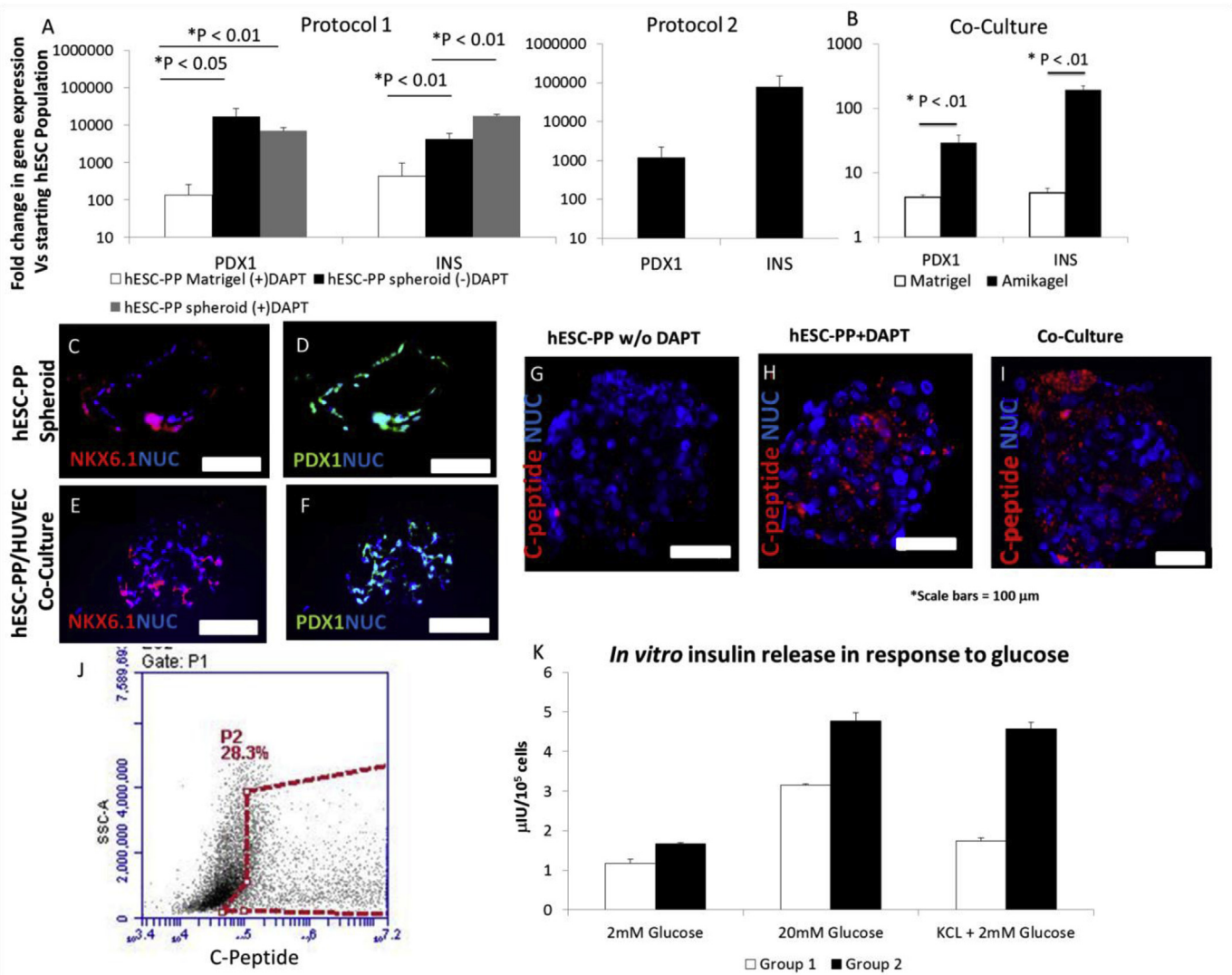


**Fig. 7.** Maturation of hESC-PP spheroid and hESC-PP/HUVEC organoids on AM<sup>3</sup> enhances islet specific maturation. (A) Gene expression levels for PDX1 and INS after chemically induced maturation on AM<sup>3</sup>. (B) PDX1 and INS gene expression of the co-cultured hESC-PP/HUVEC organoid on amikagel and matrigel. (C) Immunostaining of paraffin embedded sections showing positive NKX6.1 and (D) PDX1 protein expression (protocol 1) of hESC-PP spheroids and positive PDX1 (E) and NKX6.1 (F) protein expression in paraffin sections of the hESC-PP/HUVEC co-culture organoids. C-peptide protein expression in whole mount hESC-PP spheroids with out (G) and with DAPT (H) supplementation during maturation (protocol 1). (I) C-peptide protein expression in whole mount mature co-culture organoids. (J) Flow cytometry analysis of C-peptide positive cell population after maturation (protocol 2) (K) *In vitro* insulin release in response to glucose challenge for two trial groups of mature hESC-PP spheroids (protocol 2). All scale bars in image are 200 µm unless noted.

cultures of hESC-PP cells [51]. Here we further explored the effect of HUVEC paracrine signaling in 3D hESC-PP/HUVEC organoids, obtained by co-aggregating hESC-PP and HUVEC cells on Amikagel. Phenotypic characterization of these organoids revealed a 200-fold up-regulation of INS and 40 fold up-regulation of PDX1 gene expression (Fig. 7B) over the initial hESC-PP/HUVEC seeding population. It is additionally worth noting that these co-culture models were devoid of any specific chemical induction for maturation. Hence the observed up-regulation of INS gene in these models demonstrates that endothelial inclusion and 3D organoid formation support maturation, which also aligns with our previous report on adherent 2D cultures [51]. Parallel co-culture on Matrigel controls exhibited a much weaker effect with 5-fold increase in both PDX1 and INS gene expression over the initial seeded cell populations (Fig. 7B).

In addition to increased gene expression, immunostaining for NKX6.1 (Fig. 7C) and PDX1 (Fig. 7D) detected large populations of pancreatic endocrine cells in the matured spheroids, primarily on

the periphery. Within hESC-PP/HUVEC mature islet-like organoids, immunostaining demonstrated significant presence of NKX6.1 (Fig. 7E) and PDX1 (Fig. 7F) positive cells spread throughout the organoid. Further characterization confirmed islet specific maturation as judged by the C-Peptide immunostaining of individual whole mount aggregates (Fig. 7G–I). C-peptide expression was visibly enhanced through either chemical supplementation of DAPT in hESC-PP spheroids (Fig. 7H) or HUVEC co-culture in the organoids (Fig. 7I). Quantitative analysis of the hESC-PP spheroids matured on AM<sup>3.0</sup> by flow cytometry revealed ~30% total cell population positive for C-peptide protein (Fig. 7J). The most significant functional trait of pancreatic islets lies in their ability to secrete insulin in response to sensed glucose increases. Our organoids demonstrated significant glucose responsive insulin secretion: 3–5 µU/10<sup>5</sup> cells of insulin secretion when challenged with 20 mM glucose stimulation over ~1 µU/10<sup>5</sup> at low 2 mM glucose (Fig. 7K). These clearly demonstrate the functional maturation of the derived islet-like organoids on AM<sup>3</sup> hydrogel.

Extra-cellular matrix (ECM) produced by endocrine and supporting endothelial cell populations is critical for promoting overall islet growth, structure, and cell function [14,52]. Hence we characterized the ECM profiles within the engineered hESC-PP spheroids and heterogeneous organoids. As expected, the ECM distribution within the organoids was specific to the culture configuration (Fig. 8). ECM staining of hESC-PP aggregates revealed significant amounts of laminin and trace fibronectin and collagen IV throughout the spheroid after 2 days in culture (Fig. 8). Post-maturation the hPSC-PP spheroids developed an ECM outer layer consisting of laminin, fibronectin, and collagen IV. The inclusion of HUVEC within endothelialized organoids further exhibited a robust ECM composition throughout the interior of the aggregate with laminin, fibronectin, and collagen IV present throughout (Fig. 8).

Overall, Amikagel-induced self-aggregation of hESC-PPs in itself was sufficient to achieve pancreatic endocrine maturation, which outperformed chemically induced maturation on the Matrigel controls. Further, application of chemical induction significantly enhanced the INS gene expression and C-peptide protein expression. Inclusion of an angiocrine HUVEC population to form heterogeneous islet-like organoids resulted in spontaneous organoid maturation towards pancreatic islet like cells. Importantly, maturation in both spheroids and organoids were significantly higher than that observed in Matrigel cultures, indicating the substantial benefits of specifically engineering a controlled 3D culture configuration which was further demonstrated by functional insulin secretion in response to glucose stimulation in hESC-PP spheroids.

#### 4. Discussion

hESC's pre-differentiated to pancreatic progenitor cells spontaneously aggregated on Amikagel uniquely synthesized with a specific cross-linking concentration (AM<sup>3.0</sup>). We recently showed that an amikacin: PEG diglycidyl ether at a mole ratio of 1:3 results in the formation of multicellular spheroids with cancer cell lines [40]. Lower mole ratios of Amikacin: PEGDE (1:2 and 1:1.5) result in a predominantly adhesive Amikagel formulation [40]. Presence of non-adhesive polyethylene glycol coupled with high mechanical stiffness in the hydrogel introduced the non-adhesive property to the gel and allowed spontaneous integration of the HUVEC populations with hESC-PP cells to form islet-like organoids. The specific PEGDE to Amikacin ratio bears the appropriate chemical functionality of hydroxyl group creation that is likely conducive to promote spontaneous aggregation. These chemical moieties also allow for reproducible generation of robust and mechanically stable multicellular organoids with precise control over the organoid size, cellular composition and distribution obtained through manipulation of initial seeding population. These parameters are critical in deriving functional islet spheroids from hPSCs [14,32–34]. Specific to islet organoid generation, there is an inherent requirement for increased cell to cell communication through the 3D culture configurations and the inclusion of supporting non-endocrine cell populations for allowing complete organ derivation [14]. The 3D organoid formation on Amikagels meets both requirements which enhanced both pancreatic phenotype and its potential for islet specific maturation. The platform thus has pliability to integrate variable soluble chemical differentiation protocols as well as integrating

### *In Vitro* Extra-cellular Matrix Development in Pancreatic Organoids

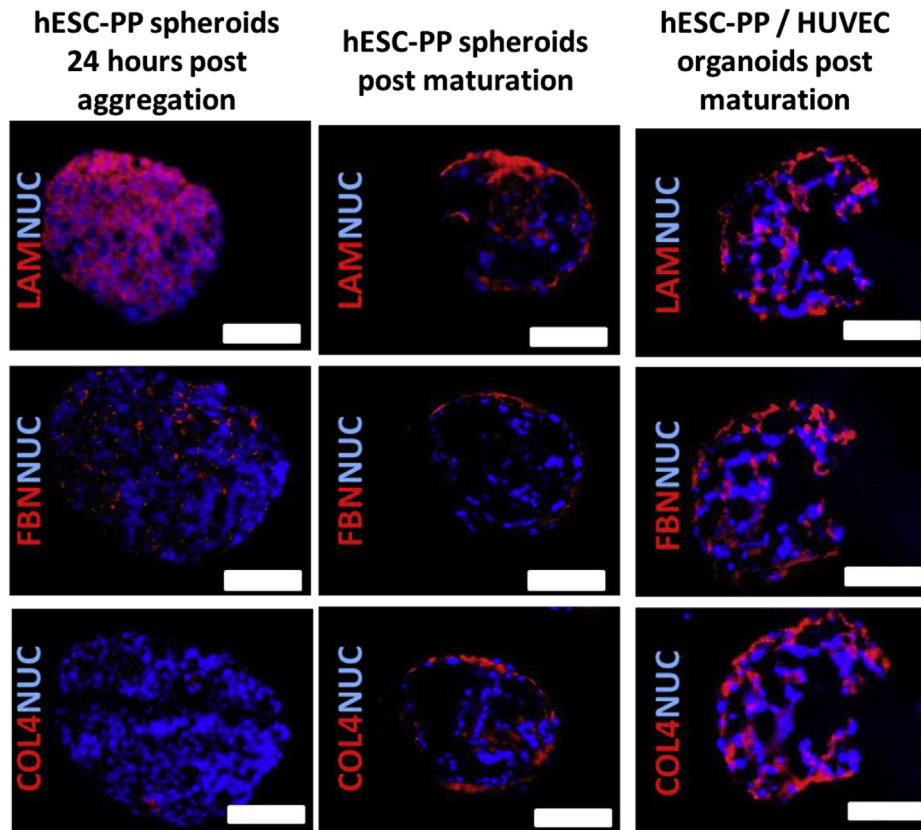


Fig. 8. Extra cellular matrix (ECM) development was located in the periphery of hPSC-PP spheroids and throughout the hPSC-PP/HUVEC mature pancreatic organoids.

supporting endothelial cell populations. Using the novel Amikagel platform, we therefore successfully generated functional beta-like cell spheroids as well as heterogeneous islet-like organoids.

Aggregation of the differentiating hESCs was dependent on two factors (i) hESC stage of maturation and (ii) Amikagel composition of the cross linked moieties. However, aggregation was not sensitive to the specific protocol for pancreatic differentiation, and hence the developed technique can be extended to new and improved future protocols. The specific integrin and cell adhesion molecules presented on the hESC surface changes with differentiation [53], which may be a direct rationale leading to the higher propensity of aggregation in hESC-PPs over less mature hESC and hESC-DE. This effect is mirrored in morphogenic events during pancreatic development and exocrine/endocrine segregation wherein CAM and cadherin expressions mediate endocrine budding from pancreatic ducts and cell sorting [54]. Within islets,  $\text{Ca}^{2+}$  dependent E-cadherin mediates cell-adhesion within the beta cell population [45], while  $\text{Ca}^{2+}$  independent CAMs such as N-CAM are primarily located in non-beta islet cell population. In our previous studies we reported an increase in both relevant E-cadherin and N-CAM gene expression with differentiation from hESC-DE to hESC-PP stage [47]. Of note, this self-aggregation behavior of hESC-PP cells was dependent on the presence of trace fetal bovine serum (2%) in the media (SI Fig. 7). The absence of serum resulted in numerous small aggregates (SI Fig. 7) scattered throughout the AM<sup>3.0</sup> gel, which could be subsequently recovered into a single spheroid by serum supplementation at a later time (SI Fig. 7).

Previous reports have also demonstrated aggregation/condensation of hPSC derived 3D organoids, explicitly driven by contractile forces generated by participating mesenchymal cells [13]. In contrast, the Amikagel surface specifically enabled robust self-aggregation of both hESC-PP cells and hESC-PP/HUVEC co-cultures independent of a stromal population. The rate of aggregation (ROA) diminishes after spheroid aggregation and the circularity factor begins to increase as the spheroid further compacts. Based on the differential adhesion hypothesis, as cells organize they form cell-cell adhesion molecules, key components of the intracellular tensile mechanisms driving cell compaction into circular spheroids. This adhesion and organization is driven by the need to minimize the surface interfacial energy of the aggregate at the expense of the Amikagel-cell integrin binding energies [13,55]. Taken together with ROA dynamics, it is hypothesized that the hESC-PP cells on AM<sup>3.0</sup> aggregate rapidly due to the added support of intracellular contractile mechanisms, which along with increased cell-cell adhesions more than compensate for the cell-Amikagel binding interactions driving the initial aggregation and later organized compaction while promoting increased systemic cell to cell interactions. While the introduction of HUVEC population may initially slow the ROA (SI Fig. 4), the ultimate organoid aggregation was successful.

The primary purpose of inducing and maintaining 3D aggregated organoids is to enhance tissue/organ specific function by reproducing the native environment, including supporting the endothelial and stromal cell populations. Three-dimensional cultures have been used to create homogenous hPSC derived islet-like spheroids which replicate native endocrine pancreatic function [32–34] using forced aggregation or matrix embedment. Various research groups, including ours, have conducted culture, propagation and pancreatic differentiation of hESCs in 2D adherent cultures [15–23] which do not recapitulate cell organization during islet development. Recently, the positive attributes of 3D culture configurations with enhanced cell-cell contact are gaining much attention [14,56], resulting in conformational shifts in hPSC culture platforms. However, current techniques for engineering islet spheroids do not allow precise control over ultimate aggregate size

or nor do they support supporting cell inclusion, which is the next progression in generating islet organoids with multi-cellular complexity and eventual generation of vascularized constructs. The Amikagel platform reported herein in this study is particularly suitable in this context by demonstrating the feasibility of spontaneous aggregation of pre-differentiated hESC-PP cells into robust spheroids with reproducible control over spatial parameters and more importantly controlled integration of supporting cell populations. The novel hydrogel permits the manipulation of partially differentiated cells to be integrated with supporting endothelial cells. ECs are closely involved in pancreatic endocrine commitment [49]. During development, pancreatic endocrine progenitors delaminate out of the pancreatic epithelium, and migrate to ECs in the vicinity. Further islet maturation coincides with islet vascularization, terminating in spheroidal islets of Langerhans [57]. The close involvement of ECs with the developing pancreas has motivated several attempts to recreate this interaction *in-vitro* [51,58,59]. Previous studies have demonstrated the feasibility of islet-specific maturation of differentiating m/h-PSCs when co-cultured with ECs [39,59]. However, to the best of our knowledge, most of these culture models are in 2D, while *in-vivo* islet organogenesis occurs in a 3D spheroid configuration.

To this end, the surface chemical structure of Amikagel allowed spontaneous integration of HUVEC populations with hESC-PP cells to form islet-like organoids, which remained fully integrated throughout the culture period. The integration of endothelial cell populations would be an important initial step towards vascular development, as demonstrated in the cancer literature [60]. In the context of regenerative medicine, tissue survival and neovessel organization of hESC derived cell populations were reported to be dependent on endothelial inclusion and mesenchymal supplementation [61]. Recently, iPSC-derived liver buds, upon co-culture with endothelial cells and stromal cells, were reported to produce immature vascular-like systems within organoids upon implantation [7,8]. In addition a developed ECM base is important for islet structure, cell health, and overall function while also being a necessary prerequisite for a developed vascular system [52]. In the current study, it was apparent that hESC-PP spheroids produced substantial laminin within 48 h of aggregation with minimal fibronectin and no collagen IV. Upon islet-specific maturation of hESC-PP spheroids, non-laminin ECM components were primarily located in a membrane surrounding the exterior of the spheroid, while laminin was also found in the spheroid interior where cavitation occurred, possibly due to lack of structural ECM support. The inclusion of supporting endothelial cells resulted in laminin, fibronectin, and collagen IV located throughout aggregate along with diminished cavitation.

Ultimately, the goal of hESC islet organoid engineering is to recapitulate organ specific functionality. 3D culture of aggregated hPSCs in a stirred suspension platform resulted in successful maturation to a high yield of  $\beta$  cell-like cells [11] and forced aggregation of hESC-PPs within a hydrogel could maintain PDX1/NKX6.1 positive populations [62]. Similarly, in this study, the same two key markers of pancreatic endocrine stage of differentiation, PDX1 and NKX6.1, gene and protein expression was significantly enhanced in hESC-PP spheroids generated on Amikagel [62,63]. Further chemical induced maturation resulted in increased INS1 gene expression and C-peptide protein expression indicative of mature  $\beta$ -cell. Interestingly, upon both 3D aggregation and integration of hESC-PP cells with HUVEC to form heterogeneous islet-like organoids supported further islet specific maturation, even in absence of specific chemical inducers. Quantification of C-peptide within hESC-PP spheroids revealed that approximately 30% of the total cell population was positive for C-peptide protein. Beyond insulin/C-peptide production, true functionality of mature islets lie

in the glucose-stimulated release of insulin. Our organoids demonstrated a functional increase of 2–4  $\mu\text{IU}/10^5$  cells of insulin at high glucose in comparison to low glucose.

## 5. Conclusions

In summary, we have described a novel Amikagel hydrogel-based platform presenting the specific amine-glycidylether coupled hydroxyl linkages conducive for inducing spontaneous aggregation of differentiating hPSCs into both homogenous and heterogeneous multi-cellular aggregates of controlled size and cellular composition. The platform utilizes cell-cell and cell-substrate interaction to facilitate cell aggregation, as opposed to imposing confinement via embedding cells in a matrix. We subsequently engineered the pancreatic islet spheroids on Amikagel which also permits, for the first time, the formation of multicellular islet 'organoids' from hESC-PPs and supporting HUVEC population. The hESC-PP spheroids had significant enhancement of cell populations co-expressing PDX1 and NKX6.1 and the 3D conformation along with endothelial introduction promoted differentiation to the endocrine pancreatic phenotype. These, in turn, contained a C-peptide positive cell population which importantly recapitulated functional glucose-stimulated insulin secretion. This unique platform thus opens up the scope of engineering complex multicellular human-specific organoids from differentiating hPSCs, involving self-organization of multiple cell types. This uniquely engineered platform also has the capacity to catalyze the next generation of vascularized human organoids for utilization in regenerative medicine and drug discovery.

## Author contributions

JC carried out all cell differentiation, biological measurements, and biological assay experiments and drafted the manuscript. KR and TSPG were responsible for the design and synthesis of Amikagel and contributed to studies on mechanical properties of the hydrogels. SKG was responsible for LICOR and confocal imaging and sample preparation. VV and ML analyzed time laps images for condensation characterization. IB, PK, KR, and JC conceived of and participated in the design of the current study on differentiation of stem cells to pancreatic organoids. IB, PK, and KR edited the manuscript. All authors approved the final manuscript.

## Competing financial interests

Dr. Taraka Sai Pavan Grandhi and Prof. Kaushal Rege are inventors of the Amikagel hydrogel technology.

## Data availability statement

The raw data required to reproduce these findings are found within the methodology and supplementary files.

## Acknowledgements

IB and KR acknowledge an NSF EAGER Grant (# 1547618) and NSF CBET Grant (#1706674) for funding this study. Authors also gratefully acknowledge the Center for Complex Engineered Multifunctional Materials (CCEMM), Swanson School of Engineering, University of Pittsburgh for providing partial financial support for this research. PNK also acknowledges the Edward R. Weidlein Chair Professorship funds and NSF (Grant # 0933153) for partial financial support of this research. KR acknowledges NIH/NIGMS (Grant 1R01GM093229-01A1) for partial financial support. RR acknowledges NSF (grant #1510700) for partial support of this study. We are

thankful to Dr. Thrimoorthy Potta for several helpful discussions relating to Amikagels.

## Appendix A. Supplementary data

Supplementary data related to this article can be found at <https://doi.org/10.1016/j.biomaterials.2018.05.031>.

## References

- [1] M.A. Lancaster, J.A. Knoblich, Organogenesis in a dish: modeling development and disease using organoid technologies, *Science* 345 (2014), 1247125.
- [2] M. Eiraku, K. Watanabe, M. Matsuo-Takasaki, M. Kawada, S. Yonemura, M. Matsumura, et al., Self-organized formation of polarized cortical tissues from ESCs and its active manipulation by extrinsic signals, *Cell Stem Cell* 3 (2008) 519–532.
- [3] M.A. Lancaster, M. Renner, C.A. Martin, D. Wenzel, L.S. Bicknell, M.E. Hurler, et al., Cerebral organoids model human brain development and microcephaly, *Nature* 501 (2013) 373–379.
- [4] T. Kadoshima, H. Sakaguchi, T. Nakano, M. Soen, S. Ando, M. Eiraku, et al., Self-organization of axial polarity, inside-out layer pattern, and species-specific progenitor dynamics in human ES cell-derived neocortex, *Proc. Natl. Acad. Sci. U.S.A.* 110 (2013) 20284–20289.
- [5] T. Nakano, S. Ando, N. Takata, M. Kawada, K. Muguruma, K. Sekiguchi, et al., Self-formation of optic cups and storable stratified neural retina from human ESCs, *Cell Stem Cell* 10 (2012) 771–785.
- [6] J.R. Spence, C.N. Mayhew, S.A. Rankin, M.F. Kuhar, J.E. Vallance, K. Tolle, et al., Directed differentiation of human pluripotent stem cells into intestinal tissue in vitro, *Nature* 470 (2011) 105–109.
- [7] T. Takebe, R.R. Zhang, H. Koike, M. Kimura, E. Yoshizawa, M. Enomura, et al., Generation of a vascularized and functional human liver from an iPSC-derived organ bud transplant, *Nat. Protoc.* 9 (2014) 396–409.
- [8] T. Takebe, K. Sekine, M. Enomura, H. Koike, M. Kimura, T. Ogaeri, et al., Vascularized and functional human liver from an iPSC-derived organ bud transplant, *Nature* 499 (2013) 481–484.
- [9] M. Takasato, P.X. Er, M. Becroft, J.M. Vanslambrouck, E.G. Stanley, A.G. Elefanti, et al., Directing human embryonic stem cell differentiation towards a renal lineage generates a self-organizing kidney, *Nat. Cell Biol.* 16 (2014) 118–126.
- [10] W. Li, R. Zhao, J. Liu, M. Tian, Y. Lu, T. He, et al., Small islets transplantation superiority to large ones: implications from islet microcirculation and revascularization, *J. Diabetes Res.* 2014 (2014), 192093.
- [11] F.W. Pagliuca, J.R. Millman, M. Gurtler, M. Segel, A. Van Dervort, J.H. Ryu, et al., Generation of functional human pancreatic beta cells in vitro, *Cell* 159 (2014) 428–439.
- [12] A. Rezaei, J.E. Bruin, P. Arora, A. Rubin, I. Batushansky, A. Asadi, et al., Reversal of diabetes with insulin-producing cells derived in vitro from human pluripotent stem cells, *Nat. Biotechnol.* 32 (2014) 1121–1133.
- [13] T. Takebe, M. Enomura, E. Yoshizawa, M. Kimura, H. Koike, Y. Ueno, et al., Vascularized and complex organ buds from diverse tissues via mesenchymal cell-driven condensation, *Cell Stem Cell* 16 (2015) 556–565.
- [14] Y. Takahashi, T. Takebe, H. Taniguchi, Engineering pancreatic tissues from stem cells towards therapy, *Regen. Ther.* 3 (2016) 15–23.
- [15] M. Jaramillo, S. Mathew, K. Task, S. Barner, I. Banerjee, Potential for pancreatic maturation of differentiating human embryonic stem cells is sensitive to the specific pathway of definitive endoderm commitment, *PLoS One* 9 (2014), e94307.
- [16] M.C. Nostro, F. Sarangi, S. Ogawa, A. Holtzinger, B. Corneo, X. Li, et al., Stage-specific signaling through TGFbeta family members and WNT regulates patterning and pancreatic specification of human pluripotent stem cells, *Development (Cambridge, England)* 138 (2011) 861–871.
- [17] A. Rezaei, J.E. Bruin, M.J. Riedel, M. Mojibian, A. Asadi, J. Xu, et al., Maturation of human embryonic stem cell-derived pancreatic progenitors into functional islets capable of treating pre-existing diabetes in mice, *Diabetes* 61 (2012) 2016–2029.
- [18] A. Rezaei, J.E. Bruin, J. Xu, K. Narayan, J.K. Fox, J.J. O'Neil, et al., Enrichment of human embryonic stem cell-derived NKX6.1-expressing pancreatic progenitor cells accelerates the maturation of insulin-secreting cells in vivo, *Stem Cell* 31 (2013) 2432–2442.
- [19] T.C. Schulz, H.Y. Young, A.D. Agulnick, M.J. Babin, E.E. Baetge, A.G. Bang, et al., A scalable system for production of functional pancreatic progenitors from human embryonic stem cells, *PLoS One* 7 (2012), e37004.
- [20] R. Xie, L.J. Everett, H.W. Lim, N.A. Patel, J. Schug, E. Kroon, et al., Dynamic chromatin remodeling mediated by polycomb proteins orchestrates pancreatic differentiation of human embryonic stem cells, *Cell Stem Cell* 12 (2013) 224–237.
- [21] K.A. D'Amour, A.G. Bang, S. Eliazar, O.G. Kelly, A.D. Agulnick, N.G. Smart, et al., Production of pancreatic hormone-expressing endocrine cells from human embryonic stem cells, *Nat. Biotechnol.* 24 (2006) 1392–1401.
- [22] E. Kroon, L.A. Martinson, K. Kadoya, A.G. Bang, O.G. Kelly, S. Eliazar, et al., Pancreatic endoderm derived from human embryonic stem cells generates glucose-responsive insulin-secreting cells in vivo, *Nat. Biotechnol.* 26 (2008)

- 443–452.
- [23] D. Zhang, W. Jiang, M. Liu, X. Sui, X. Yin, S. Chen, et al., Highly efficient differentiation of human ES cells and iPSC cells into mature pancreatic insulin-producing cells, *Cell Res.* 19 (2009) 429–438.
- [24] J. Lee, S. Lee, K. Roh, E. Jung, D. Park, A novel culture system to induce melanin synthesis by three-dimensional spheroid culture, *Biotechnol. Bioproc. Eng.* 20 (2015) 194–200.
- [25] J. Mariani, M.V. Simonini, D. Palejev, L. Tomasini, G. Coppola, A.M. Szekely, et al., Modeling human cortical development in vitro using induced pluripotent stem cells, *Proc. Natl. Acad. Sci. U. S. A.* 109 (2012) 12770–12775.
- [26] S.H. Au, M.D. Chamberlain, S. Mahesh, M.V. Sefton, A.R. Wheeler, Hepatic organoids for microfluidic drug screening, *Lab a Chip* 14 (2014) 3290–3299.
- [27] A.P. McGuigan, M.V. Sefton, Vascularized organoid engineered by modular assembly enables blood perfusion, *Proc. Natl. Acad. Sci. U. S. A.* 103 (2006) 11461–11466.
- [28] D. Zhang, M. Pekkanen-Mattila, M. Shahsavani, A. Falk, A.I. Teixeira, A.A. Herland, 3D Alzheimer's disease culture model and the induction of P21-activated kinase mediated sensing in iPSC derived neurons, *Biomaterials* 35 (2014) 1420–1428.
- [29] D. Loessner, K.S. Stok, M.P. Lutolf, D.W. Hutmacher, J.A. Clements, S.C. Rizzi, Bioengineered 3D platform to explore cell-ECM interactions and drug resistance of epithelial ovarian cancer cells, *Biomaterials* 31 (2010) 8494–8506.
- [30] K. Akeda, A. Nishimura, H. Satonaka, K. Shintani, K. Kusuzaki, A. Matsumine, Y. Kasai, K. Masuda, A. Uchida, Three-dimensional alginate spheroid culture system of murine osteosarcoma, *Oncol. Rep.* (2009) 22.
- [31] A.I. Astashkina, B.K. Mann, G.D. Prestwich, D.W. Grainger, A 3-D organoid kidney culture model engineered for high-throughput nephrotoxicity assays, *Biomaterials* 33 (2012) 4700–4711.
- [32] S.P. Raikwar, E.M. Kim, W.I. Sivit, C. Allamargot, D.R. Thedens, N. Zavazava, Human iPSC cell-derived insulin producing cells form vascularized organoids under the kidney capsules of diabetic mice, *PLoS One* 10 (2015), e0116582.
- [33] Y. Kim, H. Kim, U.H. Ko, Y. Oh, A. Lim, J.W. Sohn, et al., Islet-like organoids derived from human pluripotent stem cells efficiently function in the glucose responsiveness in vitro and in vivo, *Sci. Rep.* 6 (2016) 35145.
- [34] W. Wang, S. Jin, K. Ye, Development of islet organoids from H9 human embryonic stem cells in biomimetic 3D scaffolds, *Stem Cell. Dev.* 26 (6) (2017).
- [35] J.L. Hutter, J. Bechhoefer, Calibration of atomic-force microscope tips, *Rev. Sci. Instrum.* 64 (1993) 1868–1873.
- [36] H.-J. Butt, M. Jaschke, Calculation of thermal noise in atomic force microscopy, *Nanotechnology* 6 (1995) 1.
- [37] H. Hertz, Ueber die Berührung fester elastischer Körper, *J. Reine Angew. Math.* 92 (1882) 156–171.
- [38] R. Mahaffy, C. Shih, F. MacKintosh, J. Käs, Scanning probe-based frequency-dependent microrheology of polymer gels and biological cells, *Phys. Rev. Lett.* 85 (2000) 880.
- [39] M. Jaramillo, S. Mathew, H. Mamiya, S.K. Goh, I. Banerjee, Endothelial cells mediate islet-specific maturation of human embryonic stem cell-derived pancreatic progenitor cells, *Tissue Eng. A* 21 (2015) 14–25.
- [40] T.S.P. Grandhi, T. Potta, R. Nityanandan, I. Deshpande, K. Rege, Chemo-mechanically engineered 3D organotypic platforms of bladder cancer dormancy and reactivation, *Biomaterials* 142 (2017) 171–185.
- [41] U. Chippada, B. Yurke, N.A. Langrana, Simultaneous determination of Young's modulus, shear modulus, and Poisson's ratio of soft hydrogels, *J. Mater. Res.* 25 (2010) 545–555.
- [42] T. Takigawa, Y. Morino, K. Urayama, T. Masuda, Poisson's ratio of polyacrylamide (PAAm) gels, *Polym. Gels Netw.* 4 (1996) 1–5.
- [43] S.R. Caliari, J.A. Burdick, A practical guide to hydrogels for cell culture, *Br. J. Pharmacol.* 13 (2016) 405.
- [44] K. Urayama, T. Takigawa, T. Masuda, Poisson's ratio of poly (vinyl alcohol) gels, *Macromolecules* 26 (1993) 3092–3096.
- [45] U. Dahl, A. Sjodin, H. Semb, Cadherins regulate aggregation of pancreatic beta-cells in vivo, *Development* 122 (1996) 2895–2902.
- [46] L. Li, S.A. Bennett, L. Wang, Role of E-cadherin and other cell adhesion molecules in survival and differentiation of human pluripotent stem cells, *Cell Adhes. Migrat.* 6 (2012) 59–70.
- [47] T. Richardson, P.N. Kumta, I. Banerjee, Alginate encapsulation of human embryonic stem cells to enhance directed differentiation to pancreatic islet-like cells, *Tissue Eng. A* 20 (2014) 3198–3211.
- [48] N. Dourdin, A.K. Bhatt, P. Dutt, P.A. Greer, J.S. Arthur, J.S. Elce, et al., Reduced cell migration and disruption of the actin cytoskeleton in calpain-deficient embryonic fibroblasts, *J. Biol. Chem.* 276 (2001) 48382–48388.
- [49] E. Lammert, O. Cleaver, D. Melton, Induction of pancreatic differentiation by signals from blood vessels, *Science* 294 (2001) 564–567.
- [50] T. Shinozawa, H.Y. Yoshikawa, T. Takebe, Reverse engineering liver buds through self-driven condensation and organization towards medical application, *Dev. Biol.* 420 (2016) 221–229.
- [51] M. Jaramillo, S. Mathew, H. Mamiya, S.K. Goh, I. Banerjee, Endothelial cells mediate islet-specific maturation of human embryonic stem cell-derived pancreatic progenitor cells, *Tissue Eng. A* 21 (1–2) (2015 Jan 1) 14–25.
- [52] J.C. Stendahl, D.B. Kaufman, S.I. Stupp, Extracellular matrix in pancreatic islets: relevance to scaffold design and transplantation, *Cell Transplant.* 18 (2009) 1–12.
- [53] A.B. Prowse, F. Chong, P.P. Gray, T.P. Munro, Stem cell integrins: implications for ex-vivo culture and cellular therapies, *Stem Cell Res.* 6 (2011) 1–12.
- [54] M. Brissova, M.J. Fowler, W.E. Nicholson, A. Chu, B. Hirshberg, D.M. Harlan, et al., Assessment of human pancreatic islet architecture and composition by laser scanning confocal microscopy, *J. Histochem. Cytochem. Offic. J. Histochem. Soc.* 53 (2005) 1087–1097.
- [55] S. Sart, A.C. Tsai, Y. Li, T. Ma, Three-dimensional aggregates of mesenchymal stem cells: cellular mechanisms, biological properties, and applications, *Tissue Eng. B Rev.* 20 (2014) 365–380.
- [56] Y. Shao, J. Sang, J. Fu, On human pluripotent stem cell control: the rise of 3D bioengineering and mechanobiology, *Biomaterials* 52 (2015) 26–43.
- [57] M. Johansson, A. Andersson, P.O. Carlsson, L. Jansson, Perinatal development of the pancreatic islet microvasculature in rats, *J. Anat.* 208 (2006) 191–196.
- [58] I. Banerjee, N. Sharma, M. Yarmush, Impact of co-culture on pancreatic differentiation of embryonic stem cells, *J. Tissue Eng. Regen. Med.* 5 (2011) 313–323.
- [59] M. Jaramillo, I. Banerjee, Endothelial cell co-culture mediates maturation of human embryonic stem cell to pancreatic insulin producing cells in a directed differentiation approach, *J. Vis. Exp.* (61) (2012).
- [60] A.C. Dudley, Tumor endothelial cells, *Cold Spring Harb. Perspect. Med.* 2 (2012), a006536.
- [61] K.L. Kreutziger, V. Muskheli, P. Johnson, K. Braun, T.N. Wight, C.E. Murry, Developing vasculature and stroma in engineered human myocardium, *Tissue Eng.* 17 (2011) 1219–1228.
- [62] L.D. Amer, A. Holtzinger, G. Keller, M.J. Mahoney, S.J. Bryant, Enzymatically degradable poly(ethylene glycol) hydrogels for the 3D culture and release of human embryonic stem cell derived pancreatic precursor cell aggregates, *Acta Biomater.* 22 (2015) 103–110.
- [63] A.E. Schaffer, B.L. Taylor, J.R. Benthuisen, J. Liu, F. Thorel, W. Yuan, et al., Nkx6.1 controls a gene regulatory network required for establishing and maintaining pancreatic Beta cell identity, *PLoS Genet.* 9 (2013), e1003274.